JOTCS A
Journal of the Turkish Chemical Society
Section: A
Chemistry

TURKISH CHEMICAL SOCIETY

Preparation and *in Vitro* Adhesive Application of Visible Light-Activated Modified Sodium Alginate

Rumeysa TUTAR[1*]

[1]Department of Chemistry, Faculty of Engineering, Istanbul University-Cerrahpaşa, Avcılar, Istanbul 34320, Turkey.

Abstract: Materials that are responsive to visible light have been extensively used in biomedical applications, including tissue engineering. Tissue adhesives are among the most important applications of tissue engineering. In this study, different concentrations of Ruthenium (Ru) and sodium persulfate (SPS) photoinitiators (0.2/2, 0.5/5, and 1/10 mM) were prepared. Sodium alginate (Na-alginate) was modified with methacrylate (AlgMA) to render it photoactive. Photoactive materials prepared with different ratios of photoinitiators were physically, chemically, morphologically, and mechanically tested. The results of the different analyses supported each other. Ru/SPS concentrations of 0.2/2, 0.5/5, and 1/10 mM were used to evaluate the hydrogel structures. No physical, chemical, or mechanical differences were observed between the 0.5/5, and 1/10 mM. The in vitro adhesion properties of the hydrogels increased significantly from 0.2/2 mM to 1/10 mM Ru/SPS. As the Ru/SPS concentration was increased, a significant increase in cell viability was observed. In particular, 1/10 mM Ru/SPS showed the greatest effect and created the most statistically significant difference.

Keywords: AlgMA, Ru/SPS, Light-activation, Visible light, Tissue adhesives.

Submitted: January 22, 2025. **Accepted:** March 25, 2025.

Cite this: Tutar R. Preparation and *in Vitro* Adhesive Application of Visible Light-Activated Modified Sodium Alginate. JOTCSA. 2025;12(2): 107-16.

DOI: https://doi.org/10.18596/jotcsa.1624684

***Corresponding author's E-mail:** rumeysa.tutar@iuc.edu.tr

1. INTRODUCTION

Na-alginate is a natural anionic polysaccharide obtained from brown algae and is abundantly found on the seafloor (1-3). In brown algae, glycans include cellulose, fucans, and alginates (4). Na-alginate has excellent properties such as low cost, low cytotoxicity, and biodegradability, making it a highly attractive material for biomedical applications. Owing to these properties, it has been extensively investigated as a natural polysaccharide in various fields. Some modifications have been applied to Na-alginate structures to eliminate disadvantages, such as poor gelation and mechanical strength. In particular, hydroxyl and carboxyl groups within the molecular structure can be modified using physical, chemical, and biological methods (5). Na-alginate was processed using chemical and physical modifications. Therefore, it is possible to modify and create new alginate derivatives with controlled sequences and tailored structures.

Physical crosslinking was used to improve the properties of sodium alginate. The basic principle of physical crosslinking involves the use of hydrogen bonds and tangle points to form gel-network structures (6). In this context, ionic (Ca^{2+}) crosslinking is especially common and is formed by crosslinking and exchanging sodium ions with alginic acid. Alginate gluconate combines with gluconic acid blocks on adjacent alginic acid chains to form an eggshell pattern (7).

Chemical modification of Na-alginate can change its chemical structure. Methacrylamides and methacrylates, which are called functional labeling structures, are widely used as graft biomaterials for the photopolymerization process (8-10). Alginate has been modified with methacrylic anhydride (MA) to improve photosensitivity and adhesion strength (11). Ruthenium (Ru) is a transition metal. Ru-based transition metal complexes and sodium persulfate (SPS) have been widely used to prepare visible-light-initiation systems. Visible light at 400-700 nm has shown significant advantages in tissue-engineering applications. The Ru/SPS photoinitiator system with $\varepsilon \approx 14600\ m^{-1}\ cm^{-1}$ at 450 nm can be used most effectively in polymerization applications. In this

initiator system, Ru acted as an electron donor for SPS. Therefore, SPS accepts electrons from Ru^{2+}, which are then oxidized to Ru^{3+}. Because of these electron transfers, radicals were formed. The radicals formed here activate the photocrosslinking of methacryloyl groups in modified biomaterials (12-15).

The clinical application of tissue adhesives has gained significant attention for promoting tissue health. Suturing damaged tissue is highly challenging in terms of both patient comfort and long-term tissue healing. Furthermore, tissue adhesives have the advantages of being simple and time-saving, and can be alternatives to sutures (16-18). Understanding the chemistry of tissue materials is important for explaining the adhesion mechanisms of tissue adhesives. Therefore, Na-alginate was modified to improve its adhesion mechanism. Various tissue adhesives have been prepared and used for clinical applications. These adhesives are divided into various categories: cyanoacrylate adhesives, fibrin-based adhesives, proteins, polysaccharides, and polymer-based adhesives (18).

This study utilized the standardized test methodologies outlined by the American Society for Testing and Materials (ASTM) to perform burst pressure tests (19-20). Collagen sheets were used to mimic skin in vitro. Skin injury simulation was performed on these sheets. Tissue adhesives prepared with various photoinitiator concentrations were subjected to in vitro adhesion testing on simulated wounds. Thus, the adhesion between the material and tissue after injury and wound closure was tested in vitro. Additionally, cell viability of the tissue adhesives was tested in a cell culture study (20).

In this study, methacrylate-modified Na-alginate was prepared as a precursor material to physically and chemically crosslink the AlgMA hydrogels. The primary objective was to develop AlgMA hydrogels using varying concentrations of the Ru/SPS photoinitiator system (0.2/2, 0.5/5, and 1/10 mM) and evaluate their physical, chemical, morphological, and mechanical properties. Additionally, an in vitro skin model was simulated using collagen sheets to assess the adhesion properties of the hydrogels. These findings indicate that the concentration of the Ru/SPS photoinitiator system significantly influenced the characteristics of the resulting biostructures.

2. EXPERIMENTAL SECTION

2.1. Chemicals and Instruments

Sodium alginate, phosphate-buffered saline (PBS) tablets, methacrylic anhydride (MA), cellulose dialysis membranes (14 kDa molecular weight cut-off), tris(2,2-bipyridyl) dichlororuthenium (II) hexahydrate (Ru), and SPS were purchased from Sigma-Aldrich. The ATR-FTIR spectra of all the samples were obtained within the range of 4000 to 500 cm^{-1} using a Jasco FT/IR 6700 spectrophotometer. For NMR analysis, a JEOL ECZ500R (11.75 Tesla) spectrometer equipped with a high-performance Ultrashield™ 500 MHz superconducting magnet was utilized. Scanning electron microscopy (SEM) images were captured at various magnifications using a JEOL JSM 5600 microscope. A TA.XT Plus Texture Analysis Mechanical Tester was used for compression tests.

2.2. Synthesis of Na-Alginate-Methacryloyl (AlgMA)

Methacrylic anhydride was selected as the modification chemical to incorporate methacrylate groups into biopolymers. Sodium alginate (Na-alginate) was dissolved in DI water (2.5 wt %), and 15 ml of methacrylic anhydride per gram of alginate was added to the solution (11). The mixture was left to react for 3 h at room temperature. The reaction pH was adjusted to 7 using sodium hydroxide (NaOH). To stop the reaction, the solution was precipitated using ethanol. The precipitated polymer was then dissolved in water. Subsequently, dialysis against deionized water was performed to eliminate unreacted methacrylic anhydride. The AlgMA solution was then filtered through a filter. The purified polymer was then lyophilized under sterile conditions.

2.3. Fabrication of AlgMA Hydrogels

Dried and sterile 5 wt% AlgMA was weighed and dissolved with Ru and SPS photoinitiator systems (PI) which were prepared as 0.2mM/2mM, 0.5mM/5mM and 1mM/10mM, respectively. The prepared solutions were placed in PDMS molds (5 mm diameter × 1 mm thickness). They were then chemically crosslinked with visible light (VALO Visible Light Photocrosslinking device, Ultradent, USA) to chemically crosslink them (11-12). Various initiator concentrations at exposure times of 4 min were studied to optimize the irradiation conditions based on the PI concentrations. Then, 1M Ca^{+2} (7) was added to the crosslinked hydrogels to ionically crosslink them.

2.4. Chemical Characterization

Pristine Na-alginate, methacrylate-modified alginate, and crosslinked AlgMA hydrogels were chemically characterized by FTIR. Spectroscopic methods are preferred for defining the bonds of working molecules and elucidating their structures.

2.5. Physical Characterization

The swelling behavior of the prepared structures was determined according to a previously reported procedure (11). AlgMA solutions prepared with different photoinitiator concentrations were chemically crosslinked by curing under visible light for 240 s. It was then ionically cross-linked with 1M Ca^{+2}. The prepared structures were then frozen and lyophilized for drying. The lyophilized structures were weighed and recorded. The dry structures were then immersed in DPBS for swelling measurements. The swelling ratios at 24h and 48h were weighed and recorded. The swelling results were calculated using the following formula:

$$Swelling(\%) = (Ws - Wi)/Wi * 100 \quad (1)$$

where Wi is the initial weight and Ws is the swollen weight.

2.6. Morphological Characterization

The surface morphologies were analyzed by SEM. The samples and scaffolds were mounted on a double-sided graphite tape affixed to a metal surface and sputter-coated with gold for 10 s.

2.7. Mechanical Characterization

The materials for the mechanical characterization of the hydrogel structures were prepared as described in detail in Section 2.3. The pre-gel solution (200 µL) was used to perform the compression tests. Compression tests were applied at a strain rate of 0.6 mm min^{-1} until the failure point (maximum strain of 98%) was reached.

2.8. In vitro Burst Pressure Characterization

A standard test method was followed for the burst pressure test, ASTM standard test, F2392-04 (19). The in vitro burst pressure of the prepared hydrogels was measured using a specially designed burst pressure apparatus. Briefly, collagen sheets, which were commercially purchased and used as biological substrates, were prepared by washing with distilled water and DPBS. The wound was simulated by creating a defect in the prepared collagen sheets. Wound defects were created using a 3 mm medical punch. Next, the defective collagen sheets were placed in a burst pressure apparatus. Hydrogels with different Ru/SPS concentrations were prepared. Then, 100 µL of the prepared hydrogel was pipetted onto the defect site of the collagen sheets. The hydrogels were then cured with visible light for 4 min for chemical crosslinking and with $CaCl_2$ for 5 min for ionic crosslinking (21). The burst pressures of all the gels were recorded using a pressure sensor (PS-2017, PASCO; Roseville, CA, USA) by continuously pumping air using a flow pump (n = 4).

2.9. In vitro Cell Culture Studies

L929 Cell Line Propagation: L929 Cell Line, passage 18, was checked twice a day in T25 flasks in EMEM containing 10% FBS (Pan Biotech P30-1301) and expected to reach 70% confluency. (Doubling Time: 22-26 hours) (Cell line L929 is of ATCC CCL-1 origin). Preparation of Samples: Polymeric biogels prepared as dry samples were first kept in PBS containing 10% penicillin/streptomycin for 1 d. At the end of the waiting period, the samples were sterilized by keeping them under a UV lamp for 30 min. Cells in 96-Well Plates: 500 µL of trypsin-EDTA (Gibco, 15400054) was added to the cells that reached 70% confluence in T25 flasks and incubated at 37 °C in a 5% CO2 environment for 3-5 minutes. As soon as the cells dissociated under an inverted microscope (Zeiss Primovert, Germany), a medium containing 10% FBS was added. Centrifuge at 300xg for 5 min, and discard the medium. Add 1 mL of EMEM medium. Counting was performed on a Logos Luna II instrument using Trypan Blue (Gibco, 1525061). The polymers to be tested for cytotoxicity were added to the wells, and a medium containing 10% FBS was added so that 10^4 cells per well were added. Application of Cytotoxicity Test: Each group was made in the form of at least three replicate wells, and repeated analysis was ensured. After the material was applied, the cells waited for the time to be tested without being removed from the incubator. At the end of the hour, 10% of the well volume (equal to 20 µL of WST-8) was added to the WST-8 solution. The lights were turned off during this process. The cell culture dish was wrapped in aluminum foil and incubated for another 2 h. After 2 h, the absorbance was measured at 450 nm in a cell culture dish. The results were formulated and the percentage viability was determined (Equation 2).

$$\text{Cell Viability (\%)} = \frac{(Atreatment - Ablank)}{(Acontrol - Ablank)} * 100 \quad (2)$$

Where, A = absorbance.

2.10. Statistical Analysis

For each experiment, at least three samples were tested, and the data are presented as mean ± SD (*P < 0.05, **P < 0.01, ***P < 0.001, and ****P < 0.0001). One-way analysis of variance (ANOVA) and t-tests were performed, followed by Tukey's test for statistical analysis.

3. RESULTS AND DISCUSSION

The functional groups of Na-alginate and methacrylation-modified alginate (AlgMA) structure are shown in Figure 1. The chemical compositions of the pristine alginate and the fabricated samples were identified using FTIR spectra.

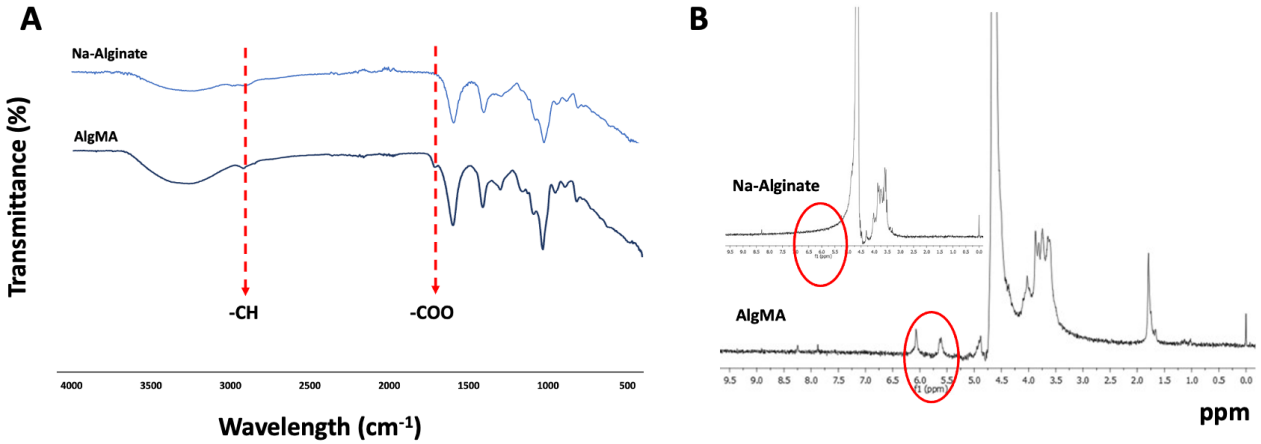

Figure 1: ATR-FTIR (A) and NMR (B) analyses of pristine alginate and AlgMA structures.

As shown in Figure 1 (A), the C=C stretching band at 1595 cm^{-1} and the C-H stretching band were observed at 2914 cm^{-1} identifying the substance. The C-H stretching peak at 2914 cm^{-1} indicated that it was an aldehyde.

When the two structures are compared in Figure 1 (A), it can be seen that the growth of the carbonyl (C=O) stretching vibration grafted with methacrylic anhydride groups showed a shoulder appearance around 1700 cm^{-1} in the AlgMA spectrum (11,21). This peak is characteristic of the methacrylate groups. In addition, νC-O bands were observed at 1296 cm^{-1}. This characteristic peak in the spectra confirms the successful modification of Na-alginate with methacrylate.

The ^{1}H-NMR spectra of Na-alginate and AlgMA are shown in Figure 1 (B). In the chemical structure formed after methacrylation, distinctive signals of groups reacting with methacrylate and vinyl groups, 5.20-6.30 ppm, were observed in the spectrum (11). In addition, Na-alginate itself does not have a significant methyl (-CH_3) group, so a significant signal around 1.75 ppm is not expected. However, for AlgMA, during the addition of the methacryloyl group, the -CH_3 (methyl) protons of the methacrylate group gave a signal around 1.75 ppm. This signal was due to the CH_3 (-C=CH_3) protons in the methacrylate group.

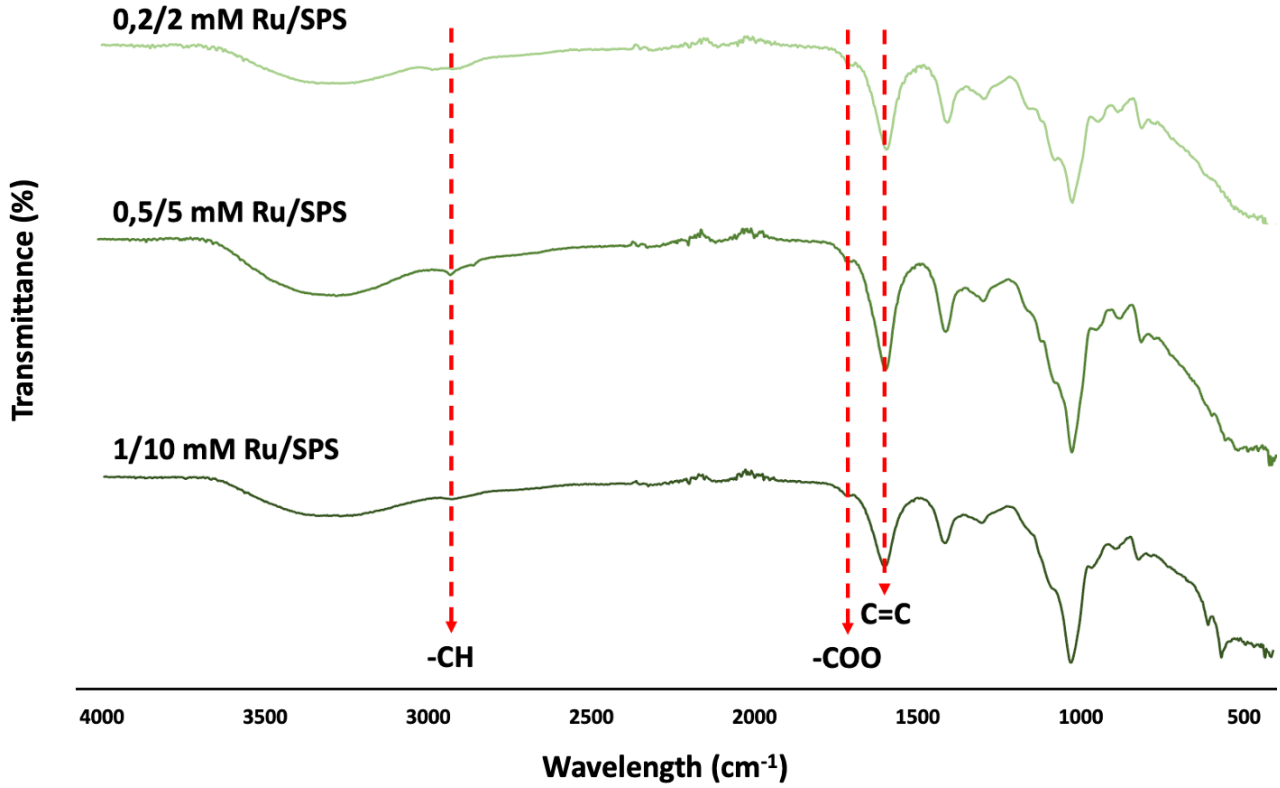

Figure 2: ATR-FTIR Analysis of AlgMA hydrogels fabricated with varying concentrations of the Ru/SPS photoinitiator.

As shown in Figure 2, the intensity of the C=C (1630-1650 cm^{-1}) peak decreased as the methacrylate groups polymerized and the double bonds opened. The C=O (1700-1750 cm^{-1}) peak does not change significantly but may become clearer as polymerization is completed. The other peak (-OH) remained constant.

The morphological characteristics of the freeze-dried hydrogel structures are shown in Figure 3. Increasing the Ru/SPS concentration increased the morphological properties of AlgMA hydrogels.

SEM images and composite elemental maps of the same structures obtained using EDS revealed that increasing the concentration of the photoinitiators influenced the porosity and pore size of the hydrogel structures. SEM analysis revealed that the AlgMA hydrogels with different photoinitiator concentrations had a homogeneous pore structure, moderately rough surface, distinct network formation, and minimal crack formation.

If the Ru ratio increases as the photoinitiator density decreases (Figure 3(A)), this may indicate that Ru is concentrated (tends to cluster) in certain regions. The decrease in the atomic value (%) of Ru from 12.7 (Figure 3(B)) to 2.4 (Figure 3(C)) indicates that the Ru concentration in the sample decreases. If the Ru ratio decreases as the photoinitiator density increases, this may indicate that Ru is more dispersed or that cross-linking increases.

For the scaffolds prepared with 0.5/5 mM and 1/10 mM Ru/SPS systems (Figure 3(B-C)), the pores are almost homogeneous and regular, which indicates that the material has undergone a controlled production process.

Alginate-based materials form a specific network structure as a result of crosslinking (ionic crosslinking with calcium and covalent bonding with visible light). The free-radical crosslinking reaction rate increases as the concentration of the Ru/SPS system increases, which increases the formation of covalent crosslink bonds (22).

The swelling properties of the AlgMA hydrogels are shown in Figure 4.

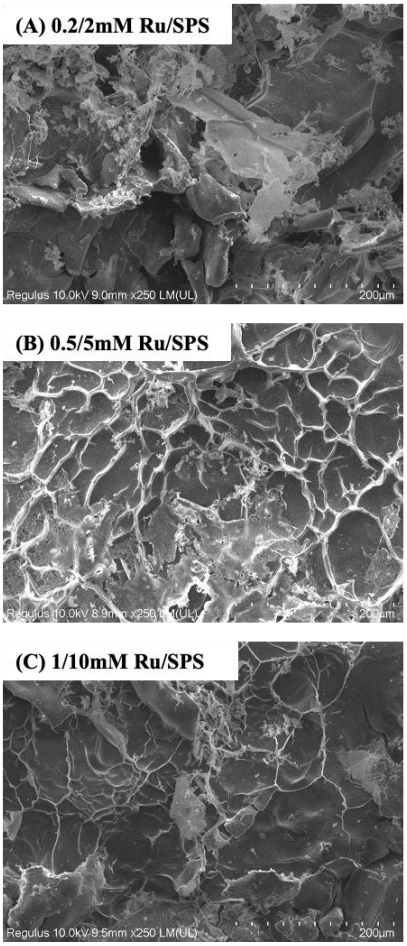

Element	Atomic %	Atomic % Error	Weight %	Weight % Error
C	8.7	0.0	4.4	0.0
N	1.3	0.1	0.8	0.1
O	80.3	0.2	53.9	0.2
S	0.1	0.0	0.1	0.0
Ru	9.6	0.0	40.8	0.1

Element	Atomic %	Atomic % Error	Weight %	Weight % Error
C	3.2	0.0	1.5	0.0
N	0.2	0.1	0.1	0.0
O	83.7	0.2	50.1	0.1
S	0.2	0.0	0.2	0.0
Ru	12.7	0.0	48.2	0.1

Element	Atomic %	Atomic % Error	Weight %	Weight % Error
C	30.0	0.1	21.4	0.1
N	3.5	0.2	2.9	0.2
O	63.7	0.2	60.6	0.2
S	0.3	0.0	0.6	0.0
Ru	2.4	0.0	14.5	0.0

Figure 3: SEM images and Energy Dispersive Spectroscopy (EDS) analysis of AlgMA hydrogels fabricated with varying concentrations of Ru/SPS photoinitiator. Scale bar: 200 μm.

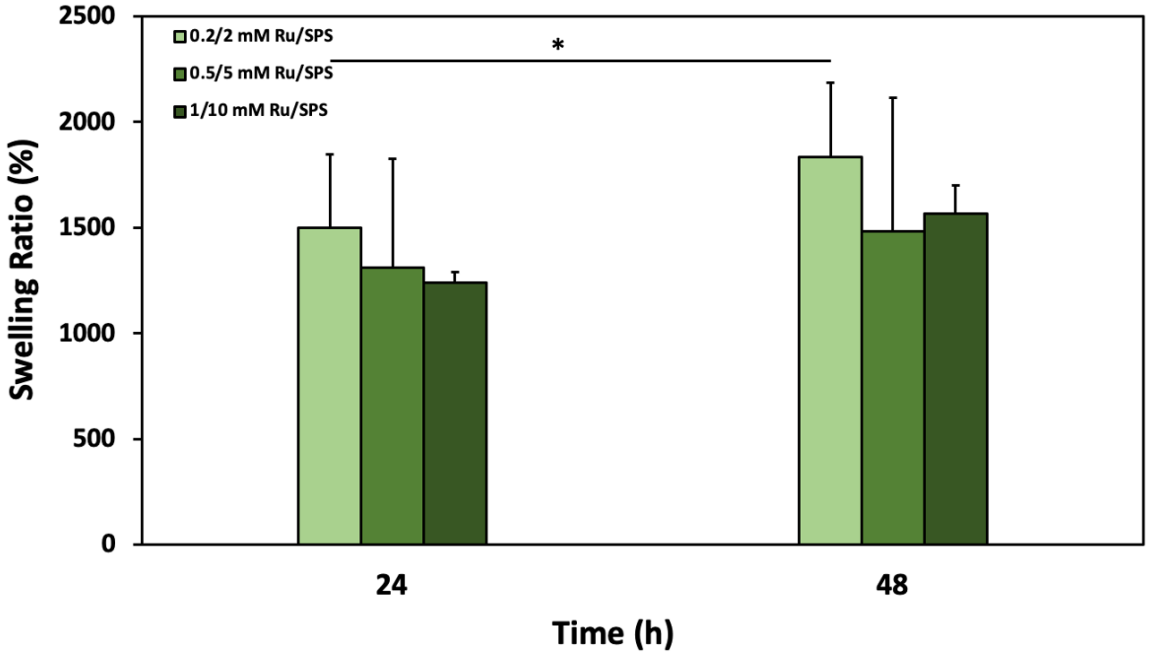

Figure 4: Swelling properties of AlgMA hydrogels fabricated with varying concentrations of the Ru/SPS photoinitiator (n=4).

Measurements at 24h and 48h showed that increasing the initiator concentration from 0.2/2 mM Ru/SPS to 0.5/5 or 1/10 mM Ru/SPS did not cause any significant difference in the swelling ratio. These results indicate that 0.2/2 mM Ru/SPS is sufficient to complete the cross-linking of the monomers. Again, the swelling behavior at 24h and 48h did not show any significant change for the 0.5/5 mM and 1/10 mM Ru/SPS systems. Moreover, the–OH groups in Na-alginate were transferred to -COO via a methacrylate modification reaction, which also limited the water absorption ability.

The stiffness of the fabricated AlgMA hydrogel was measured. The compressive modulus and compressive strength of AlgMA hydrogels synthesized with varying concentrations of the Ru/SPS photoinitiator system are presented in Figure 5.

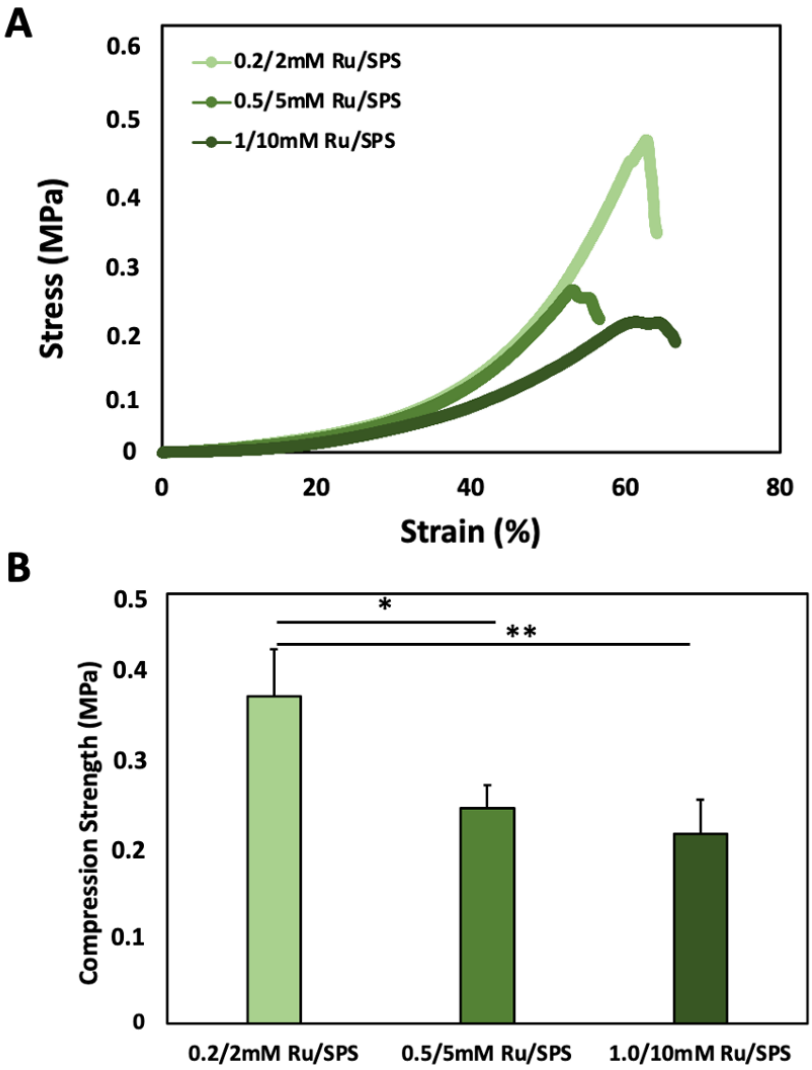

Figure 5: Compressive modulus (A) and strength (B) of AlgMA hydrogels fabricated using different concentrations of Ru/SPS (n=3).

As shown in Figure 5A, the 0.2/2 mM Ru/SPS sample appears to have a higher load-carrying capacity compared to the others, reaching the highest stress value (strength increase). All samples initially exhibited elastic deformation at low strains. Moreover, the 0.2/2 mM Ru/SPS sample shows a sudden fracture at approximately 60% strain, whereas the other samples break with lower strength or exhibit yielding behavior. In addition, it can be observed that as the Ru/SPS concentration increased, the material carried lower stress and exhibited earlier deformation.

Hydrogels prepared using 0.2/2 mM Ru/SPS (0.44 ± 0.05 MPa) exhibited a significantly higher compressive modulus than those fabricated with 0.5/5 mM (0.27 ± 0.03 MPa) and 1/10 mM (0.26 ± 0.04 MPa) Ru/SPS. However, no statistically significant differences were observed when the Ru/SPS concentration was increased to 0.5/5 mM or 1/10 mM. These findings suggest that a concentration of 0.2/2 mM Ru/SPS is sufficient to achieve complete crosslinking of the AlgMA macromers (Figure 5B).

These data show that a low concentration of 0.2/2 mM Ru/SPS offers the best mechanical performance; however, the elastic modulus and strength decrease as the concentration increases. If more strength is desired, it may be necessary to optimize the

crosslinking structure or improve the mechanical properties of the material through different modifications.

ASTM standards for biological adhesive hydrogels were used in the experiments. A collagen sheet, which was commercially purchased and used as the biological substrate, was prepared (Figure 6 (A)). The wound was then simulated by creating a defect in the prepared collagen sheets (Figure 6 (B)). Wound defects were created using a 3 mm medical punch. Next, the defective collagen sheets were placed in a burst pressure apparatus. AlgMA solutions prepared with different Ru/SPS concentrations were then added to the wound defects, as shown in Figure 6 (C). After the addition of the AlgMA solutions, they were covalently cross-linked with visible light (Figure 6 (D)). Then, ionic cross-linking with Ca^{+2} was performed to prepare the AlgMA hydrogel for the study.

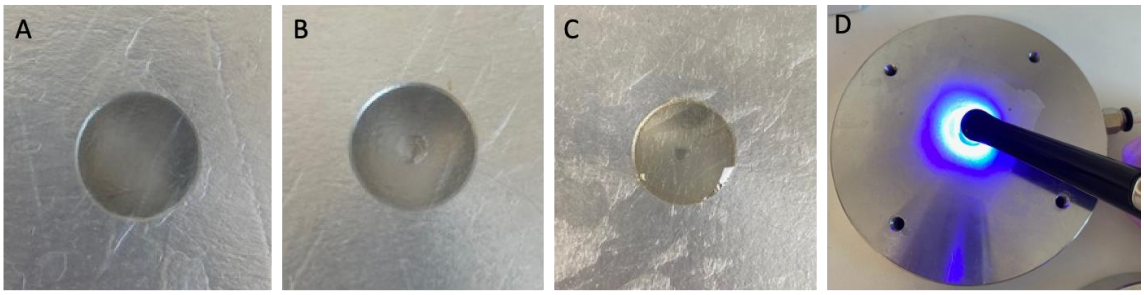

Figure 6: Images of AlgMA Hydrogels for adhesive application to a collagen sheet. Collagen sheet in the burst pressure apparatus (A), wound defect on the sheet (B), AlgMA solution (C), and cross-linking with visible light (D).

Various photoinitiator concentrations at an exposure time of 4 min. Then, 1M $CaCI_2$ was added to the crosslinked hydrogels to ionically crosslink them.

An in vitro burst pressure test was performed (Figure 7) to demonstrate how the adhesion properties changed with the different photoinitiator concentrations. A low photoinitiator concentration negatively affected AlgMA adhesion properties. After applying pressure, the material was separated from the collagen layer in a short time of 20 seconds.

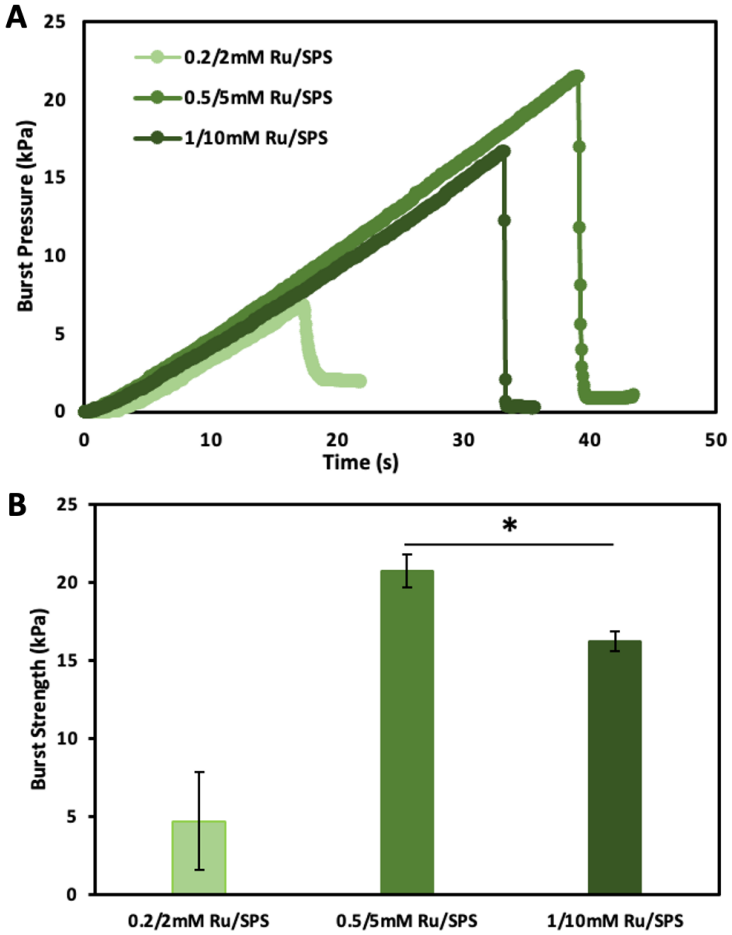

Figure 7: In vitro adhesive properties, burst pressure (A), and burst strength (B) of AlgMA hydrogels.

In Figure 7(A), 0.2/2 mM Ru/SPS reached the lowest burst pressure and failed in approximately 20 s, whereas 0.5/5 mM Ru/SPS and 1/10 mM Ru/SPS samples withstood higher pressures (around 20 kPa) and burst in approximately 30-40 seconds. In addition, the 1/10 mM Ru/SPS exhibited the highest strength. In all samples, the pressure increased linearly, and when it reached a certain threshold point, a sudden drop occurred, resulting in sample destruction. Higher burst pressures and longer durations were observed at higher concentrations.

This indicates that the interaction between the material and collagen was insufficient. As the photoinitiator concentration increased, the adhesion strength also increased. However, as the concentration increased, the material strength increased, as the AlgMA-cured areas were completely cured, which slightly reduced the adhesion strength with the collagen layer. The burst pressures of hydrogels significantly increased from 4.7 ± 3.11 kPa to 20.75 ± 1.06 kPa and 16.25 ± 0.6 kPa as the photoinitiator concentration was increased from 0.2/2 mM to 1/10 mM Ru/SPS concentration (Figure 7(B)).

As the Ru/SPS concentration increased, the resistance of the material to the burst pressure increased. Ru/SPS (1/10 mM) showed the best mechanical performance, whereas 0.2/2 mM Ru/SPS exhibited the lowest strength. This indicates that a higher degree of crosslinking or network density increased the mechanical strength of the material.

Different concentrations of the Ru/SPS system resulted in viability and abundance of live cells (Figure 8) at 24h.

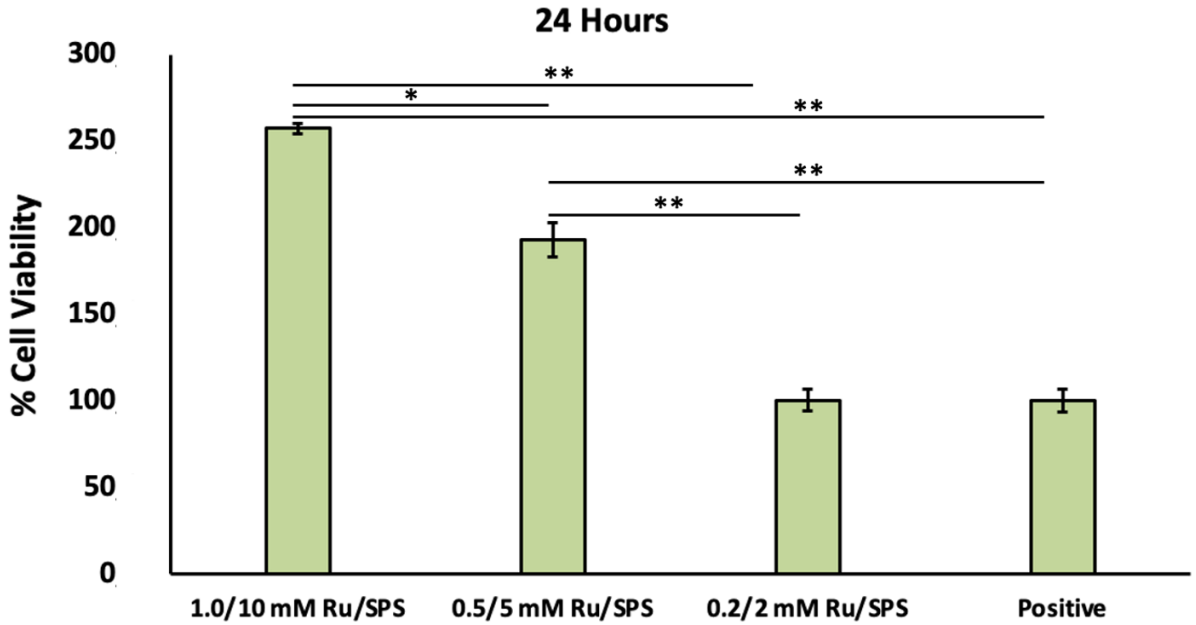

Figure 8: Viability and metabolic activity of fibroblasts cultured on AlgMA Hydrogels after 24h. (*p<0.05, mean±std, n=3) All analyses were performed in triplicate.

When the cell study results were evaluated, a significant increase in cell viability was observed with increasing Ru/SPS concentration. At the end of the 24-h incubation period, cell viability rates were at the highest level in the 1.0/10 mM Ru/SPS group, while a relatively lower but still high value was observed in the 0.5/5 mM Ru/SPS group. Cell viability in the 0.2/2 mM Ru/SPS group decreased significantly and fell to a level closer to the positive control (L929 Cell Line) group. These results reveal the dose-dependent effect of Ru/SPS concentration on cell viability (23).

4. CONCLUSION

In this study, different concentrations of the Ru/SPS photoinitiator (0.2/2, 0.5/5, and 1/10 mM) were prepared. Na-alginate was selected as the biomaterial and was modified with methacrylate to make it photoactive. Photoactive AlgMA hydrogels prepared using different ratios of photoinitiators were tested physically, chemically, morphologically, mechanically, and biologically. AlgMA hydrogels with 0.2/2 mM Ru/SPS and 0.5/5 or 1/10 mM Ru/SPS did not cause any significant differences in the swelling ratio. However, increasing the Ru/SPS concentration positively affects the homogeneity of the hydrogel structures. The scaffolds prepared with the 0.5/5 mM and 1/10 mM Ru/SPS systems exhibited homogeneity and regularity, indicating that the material underwent a controlled production process. The hydrogels prepared using 0.2/2 mM Ru/SPS exhibited a significantly higher compressive modulus, comparable to those fabricated with 0.5/5 mM and 1/10 mM Ru/SPS. However, no statistically significant differences were observed when the Ru/SPS concentration was increased to 0.5/5 mM or 1/10 mM. The in vitro adhesion properties of hydrogels significantly increased from 4.7 ± 3.11 kPa to 20.75 ± 1.06 kPa and 16.25 ± 0.6 kPa as the photoinitiator concentration was increased from 0.2/2 mM to 1/10 mM Ru/SPS concentration. As the Ru/SPS concentration was increased, a significant increase in cell viability was observed. In particular,

1/10 mM Ru/SPS showed the greatest effect and created the most statistically significant difference.

5. CONFLICT OF INTEREST

The author declares that she has no affiliations with or involvement in any organization or entity with any financial interest in the subject matter or materials discussed in this manuscript.

6. REFERENCES

1. Sellimi S, Younes I, Ayed H Ben, Maalej H, Montero V, Rinaudo M, et al. Structural, physicochemical and antioxidant properties of sodium alginate isolated from a Tunisian brown seaweed. Int J Biol Macromol [Internet]. 2015 Jan 1;72:1358–67. Available from: <URL>.

2. Rinaudo M. Main properties and current applications of some polysaccharides as biomaterials. Polym Int [Internet]. 2008 Mar 9;57(3):397–430. Available from: <URL>.

3. Ishikawa K, Miyamoto Y, Takechi M, Toh T, Kon M, Nagayama M, et al. Non-decay type fast-setting calcium phosphate cement: Hydroxyapatite putty containing an increased amount of sodium alginate. J Biomed Mater Res [Internet]. 1997;36(3):393–9. Available from: <URL>.

4. Rinaudo M. Seaweed polysaccharides, in Comprehensive Glycoscience, vol. 4, ed. by Kamerling JP. Elsevier. In Amsterdam, Netherlands; 2007. p. 691–735.

5. Szekalska M, Puciłowska A, Szymańska E, Ciosek P, Winnicka K. Alginate: Current use and future perspectives in pharmaceutical and biomedical applications. Int J Polym Sci [Internet]. 2016 Jan 1;2016(1):7697031. Available from: <URL>.

6. Paul UC, Manian AP, Široká B, Duelli H, Bechtold T. Sorption of iron(III)–alginate complexes on cellulose fibres. Cellulose [Internet]. 2013 Oct 6;20(5):2481–90. Available from: <URL>.

7. Dhamecha D, Movsas R, Sano U, Menon JU. Applications of alginate microspheres in therapeutics delivery and cell culture: Past, present and future. Int J Pharm [Internet]. 2019 Oct 5;569:118627. Available from: <URL>.

8. Sun F, Guo J, Liu Y, Yu Y. Preparation, characterizations and properties of sodium alginate grafted acrylonitrile/polyethylene glycol electrospun nanofibers. Int J Biol Macromol [Internet]. 2019 Sep 15;137:420–5. Available from: <URL>.

9. Vuocolo T, Haddad R, Edwards GA, Lyons RE, Liyou NE, Werkmeister JA, et al. A highly elastic and adhesive gelatin tissue sealant for gastrointestinal surgery and colon anastomosis. J Gastrointest Surg [Internet]. 2012 Apr 1;16(4):744–52. Available from: <URL>.

10. Lim KS, Klotz BJ, Lindberg GCJ, Melchels FPW, Hooper GJ, Malda J, et al. Visible light cross-linking of gelatin hydrogels offers an enhanced cell microenvironment with improved light penetration depth. Macromol Biosci [Internet]. 2019 Jun 26;19(6):1900098. Available from: <URL>.

11. Tutar R, Ceylan D, Çelebi-Saltik B. Preparation and characterization of conductive and multi-network nanocomposite hydrogels as potential scaffolds for electroactive tissues. New J Chem [Internet]. 2024 Aug 19;48(33):14736–45. Available from: <URL>.

12. Annabi N, Rana D, Shirzaei Sani E, Portillo-Lara R, Gifford JL, Fares MM, et al. Engineering a sprayable and elastic hydrogel adhesive with antimicrobial properties for wound healing. Biomaterials [Internet]. 2017 Sep 1;139:229–43. Available from: <URL>.

13. Lim KS, Ramaswamy Y, Roberts JJ, Alves M, Poole-Warren LA, Martens PJ. Promoting cell survival and proliferation in degradable poly(vinyl alcohol)–tyramine hydrogels. Macromol Biosci [Internet]. 2015 Oct 11;15(10):1423–32. Available from: <URL>.

14. Fancy DA, Denison C, Kim K, Xie Y, Holdeman T, Amini F, et al. Scope, limitations and mechanistic aspects of the photo-induced cross-linking of proteins by water-soluble metal complexes. Chem Biol [Internet]. 2000 Sep 1;7(9):697–708. Available from: <URL>.

15. Lim KS, Levato R, Costa PF, Castilho MD, Alcala-Orozco CR, van Dorenmalen KMA, et al. Bio-resin for high resolution lithography-based biofabrication of complex cell-laden constructs. Biofabrication [Internet]. 2018 May 11;10(3):034101. Available from: <URL>.

16. Bouten PJM, Zonjee M, Bender J, Yauw STK, van Goor H, van Hest JCM, et al. The chemistry of tissue adhesive materials. Prog Polym Sci [Internet]. 2014 Jul 1;39(7):1375–405. Available from: <URL>.

17. Duarte AP, Coelho JF, Bordado JC, Cidade MT, Gil MH. Surgical adhesives: Systematic review of the main types and development forecast. Prog Polym Sci [Internet]. 2012 Aug 1;37(8):1031–50. Available from: <URL>.

18. Spotnitz WD, Burks S. Hemostats, sealants, and adhesives: components of the surgical toolbox. Transfusion [Internet]. 2008 Jul 8;48(7):1502–16. Available from: <URL>.

19. ASTM F2392-04, 2015, ASTM International, West Conshohocken, PA [Internet]. Available from: <URL>.

20. Tutar R, Yüce-Erarslan E, İzbudak B, Bal-Öztürk A. Photocurable silk fibroin-based tissue sealants with enhanced adhesive properties for the treatment of corneal perforations. J Mater Chem B [Internet]. 2022 Apr 13;10(15):2912–25. Available from: <URL>.

21. Tavafoghi M, Sheikhi A, Tutar R, Jahangiry J, Baidya A, Haghniaz R, et al. Engineering tough, injectable, naturally derived, bioadhesive composite

hydrogels. Adv Healthc Mater [Internet]. 2020 May 24;9(10):1901722. Available from: <URL>.

22. Kim H, Jang JH, Han W, Hwang HJ, Jang J, Kim JY, et al. Extracellular matrix-based sticky sealants for scar-free corneal tissue reconstruction. Biomaterials [Internet]. 2023 Jan 1;292:121941. Available from: <URL>.

23. Murphy CM, Haugh MG, O'Brien FJ. The effect of mean pore size on cell attachment, proliferation and migration in collagen–glycosaminoglycan scaffolds for bone tissue engineering. Biomaterials [Internet]. 2010 Jan 1;31(3):461–6. Available from: <URL>.